Desalination and Water Treatment
www.deswater.com
doi: 10.5004/dwt.2022.28562

264 (2022) 121–132
July

Preparation, characterization, and adsorption performance of activated rice straw as a bioadsorbent for Cr(VI) removal from aqueous solution using a batch method

Adewirli Putra[a,b], Syiffa Fauzia[c], Deswati[d], Syukri Arief[e], Rahmiana Zein[a,*]

[a]*Laboratory of Analytical Environmental Chemistry, Department of Chemistry, Andalas University, Padang 25163, West Sumatera, Indonesia, Tel. +62751-71671; Fax: +62751-73118; emails: mimiedison@yahoo.co.id/rzein@sci.unand.ac.id (R. Zein), adewirliputra@gmail.com (A. Putra)*
[b]*Laboratory of Chemistry, Department of Medical Laboratory Technology, College of Health Sciences Syedza Saintika, Padang 25132, West Sumatera, Indonesia*
[c]*Research Center for Chemistry, National Research and Innovation Agency, Jakarta, 10340 Indonesia, Tel. +62 21-3169010; email: syiffa.fauzia@brin.go.id (S. Fauzia)*
[d]*Laboratory of Applied Chemistry, Department of Chemistry, Andalas University, Padang 25163, West Sumatera, Indonesia, Tel. +62751-71671; Fax: +62751-73118; email: deswati_ua@yahoo.co.id (Deswati)*
[e]*Laboratory of Material Chemistry, Department of Chemistry, Andalas University, Padang 25163, West Sumatera, Indonesia, Tel. +62751-71671; Fax: +62751-73118; email: syukriarief@yahoo.com (S. Arief)*

Received 9 November 2021; Accepted 12 May 2022

ABSTRACT

This research investigated the adsorption of Cr(VI) using HNO_3 0,01 M-activated rice straw in a batch system. Some parameters such as pH, initial Cr(VI) concentration, and contact times were examined. The optimum conditions were achieved at the pH 3, initial Cr(VI) concentration 800 mg/L in 15 min with adsorption capacity 60.204 mg/g. It was found that the adsorption of Cr(VI) onto activated rice straw was followed the Freundlich isotherm model (R^2 = 0.9957) and pseudo-second-order model (R^2 = 0.9995) indicating that adsorption chemically occurred and multilayer. Whereas the thermodynamic study revealed that Cr(VI) adsorption onto activated rice straw was exothermic ($\Delta H°$ = –8.658 kJ/mol) non-spontaneous reaction ($\Delta G°$ = positive) with liquid/solid interface disorder ($\Delta S°$ = –65,297 J/mol). The physicochemical characterization of the bioadsorbent showed a wavenumber shifting of some functional groups. The percentage of Cr(VI) in bioadsorbent increased and the surface morphology of the bioadsorbent was smoother after adsorption occurred. Thus, this locally abundant rice straw could be used as a bioadsorbent for Cr(VI) removal.

Keywords: Activated rice straw; Adsorption; Batch method; Cr(VI); Isotherms; Kinetics

1. Introduction

In the last decades, wastewater containing heavy metals has become a world concern [1,2]. Chromium is one of the heavy metals that could threaten the environment and human health. Chromium exists in several oxidation states: Cr(VI) and Cr(III). Cr(III) was less harmful than Cr(VI) [3]. Exposure to Cr(VI) can cause tubular swelling, severe necrosis of the kidneys, stomach, impaired liver function, and cause lung cancer [4,5]. The maximum limit of chromium that is allowed according to the standards of EPA [5], WHO [6], and Permenkes RI No.32 of 2017 [7] is 0.05 mg/L for drinking water; 0.1 mg/L, surface or groundwater, and 0.25 mg/L for industrial water. Recently,

* Corresponding author.

common methods for removing Cr(VI) from water and industrial effluents include electrocoagulation [8], electrochemical ion-exchange [9], photocatalytic reduction [10] and membrane filtration [11]. Unfortunately, those mentioned methods have some drawbacks such as high cost, complicated and need advanced technology [12]. Thus, an alternative approach was required to replace those mentioned methods. An adsorption method as an alternative method offered several advantages such as efficient, effective, and low cost because it utilized biomass waste as an adsorbent for pollutant removal in the solution [13,14]. Some previous studies have reported the application of bioadsorbent for Cr(VI) removal such as neem bark powder [15], aminated rice straw-grafted-poly(vinyl alcohol) (A-RS/PVA) [16], mucilaginous seeds of *Cydonia oblonga* [17], amine-functionalized modified rice straw [18], *Bauhinia rufescens* [19], sagwan sawdust biochar [20], Magnolia leaf [21], etc.

Rice straw is a by-product of the rice-growing process, which plays an important role in the world's food supply. In Indonesia, the production capacity of rice straw was estimated to be close to 106 million tons per year [22]. However, it has not been used optimally, which has the potential to be converted into large amounts of bioadsorbent. Many researchers started to pay attention to this type of agricultural waste to increase its economic, social, and environmental benefits [23]. Rice straw is a biomaterial with high and distinctive fiber such as the lignocellulosic group rich in cellulose, hemicellulose, lignin, and silica. The rice straw consists of 32.0%–38.6% cellulose, 19.7%–35.7% hemicellulose, 13.5%–22.3% lignin, 10%–17% ash, and 70.8% silica [24,25]. These compounds have many active groups such as hydroxyl, carbonyl, carboxyl groups, and others, playing an active site in the adsorption process and giving a flocculation effect with heavy metals [26,27].

The utilization of rice straw coming from various places such as China [27,28] India [29] as bioadsorbent for Cr(VI) ions removal has been reported. But the utilization of rice straw originated from Tarusan, West Sumatera, Indonesia, which was acid-modified, has not been reported yet**.** The location, type of soil, and climate affected rice straw's chemical composition, providing different characteristics in Cr(VI) removal [30]. Thus, this research was aimed to investigate the ability of local rice straw that has been activated by HNO_3 for removing Cr(VI) ions from aqueous solution. This research also studied the parameters affecting Cr(VI) adsorption onto activated rice straw such as pH, initial Cr(VI) concentration and predicted its mechanism by investigating isotherm, kinetic thermodynamic, physical, and chemical characterization bioadsorbent.

2. Experimental

2.1. Materials

Rice straw (*Oryza sativa*) was collected from Tarusan, Pesisir Selatan, West Sumatra, Indonesia. All chemicals such as potassium dichromate ($K_2Cr_2O_7$), nitric acid (HNO_3), sodium hydroxide (NaOH), and buffer solution (pH 2–6) were supplied by Merck as analytical grade. All reagents were dissolved in distilled water.

2.2. Bioadsorbent preparation and characterization

The rice straw was rinsed and dried at room temperature for ±2 weeks. Later, the rice straw was cut into smaller pieces (2–3 cm), ground, and the powder was sieved with size ≥36 μm. Then the bioadsorbent was soaked into HNO_3 0.01 M with a ratio of 1:3 for 120 min. After that, the bioadsorbent was filtered and rinsed until neutral pH was reached. The powder was dried and sieved using the same size sieving. The bioadsorbent was ready for further use. The characterization of bioadsorbent was done using Fourier-transform infrared spectroscopy (FTIR) (Unican Mattson Mod 7000), X-ray fluorescence (XRF, PANalytical Epsilon 3), scanning electron microscopy with energy-dispersive X-ray spectroscopy (SEM-EDX, Hitachi S-3400N), and thermogravimetric analysis (TGA, Linseiss, Type: STA PT 360).

2.3. Point zero charge adsorption study

0.1 M KCl with various pH (2–7) was prepared by adding 0.01 M HNO_3 or 0.01 M NaOH. 0.1 g of bioadsorbent was added into 25 mL of each 0.1 M KCl solution and stirred for 24 h with an agitation speed of 100 rpm. The curve was made by connecting pHo (initial pH) vs. ΔpH (change in pH) [31].

2.4. Biosorption study

0.1 g of bioadsorbent was added into 10 mL of Cr(VI) solution in Erlenmeyer flask 25 mL. The experimental conditions were set at the different variations of parameters (pH 2–6, Cr(VI) initial concentration 100–1,400 mg/L, contact time 15–90 min, and temperature 298–318 K). The agitation rate was 100 rpm with particle size ≥36 μm. The concentration of metal ions before and after adsorption was measured by Atomic Absorption Spectrophotometer (AA240) at the wavenumber 429 nm [31]. The adsorption capacity and adsorption efficiency were calculated by the following Eqs. (1) and (2):

$$\text{Adsorption Capacity, } q = \frac{\left(C_o - C_e\right)V}{m} \tag{1}$$

$$\text{Adsorption Efficiency, } \%R = \frac{\left(C_o - C_e\right)}{C_o} \times 100\% \tag{2}$$

where C_o and C_e (mg/L) were initial and equilibrium concentrations of Cr(VI). V (L) was the volume of Cr(VI) ion solution and m (g) was the mass of bioadsorbent.

3. Results and discussion

3.1. Bioadsorbent characterization

3.1.1. FTIR and XRF analysis

Rice straw was characterized using FTIR within wavenumber 4,000–450 cm^{-1}. FTIR analysis provided information regarding functional groups involved in Cr(VI) sorption and predicted the mechanism between bioadsorbent and

adsorbate [32]. Fig. 1 shows that the functional groups existed in rice straw. The wavenumber at 3,861.14 cm^{-1} indicated N–H stretching. The broad peak at 3,400.31 cm^{-1} was O–H stretching, and the peak at 2,918.03 cm^{-1} described C–H aliphatic, the peak at 2,850.28 cm^{-1} indicated C–H stretching of aldehyde. Meanwhile, C=O stretching and C=C were shown at 2,352.06 and 1,653.06 cm^{-1}, respectively. C–NO_2 aromatic stretching was indicated at 1,516.92 cm^{-1}. The peak at 1,320.08 and 1,104.51 cm^{-1} represented C=O stretching and Si–O, respectively. Those mentioned peaks revealed the complexity of bioadsorbent properties and played an important role in adsorption [33]. The FTIR spectra of activated rice straw showed some missing peaks due to HNO_3 0.01M activation. The missing peaks included N–H stretching at 3,861.14 cm^{-1}, C–H stretching at 2,850.28 cm^{-1}, C=O stretching at 2,352.06 cm^{-1}. The wavenumber of some peaks even shifted due to the activation process. The FTIR spectra of activated rice straw after adsorption revealed a shifting of each functional group (Table 1). This shifting indicated an interaction between functional groups and Cr(VI) ions [20,34,35].

From the results of the characterization using XRF, the chemical composition of the bioadsorbent (Table 2) changed after the adsorption of Cr(VI) ions. The percentage of some elements and metal oxides decreased after adsorption occurred, such as Mg, K, Cl, MgO, K_2O, and others. It indicated that, under acidic conditions (pH 3), some metal oxides on the surface of the bioadsorbent dissolved. The presence of a functional group (electron donor), which has a lower reduction potential value, caused Cr(VI) ion (anion) to be reduced to Cr(III) (cation) [Eq. (3)]. So that the Cr(III) ion forms a complex compound with a functional group and ion exchange between Cr(III) and Ca^{2+}, Mg^{2+}, K^+ on the surface of the bioadsorbent [27].

$$Cr_2O_7^{2-} + 14H^+ + 6e \rightarrow 2Cr^{3+} + 7H_2O \quad (3)$$

In acidic conditions, the bioadsorbent surface underwent protonation that later provoked Cl^- ion releasing from the bioadsorbent surface. Then it was followed by electrostatic interaction between anionic species ($HCrO_4^-$,

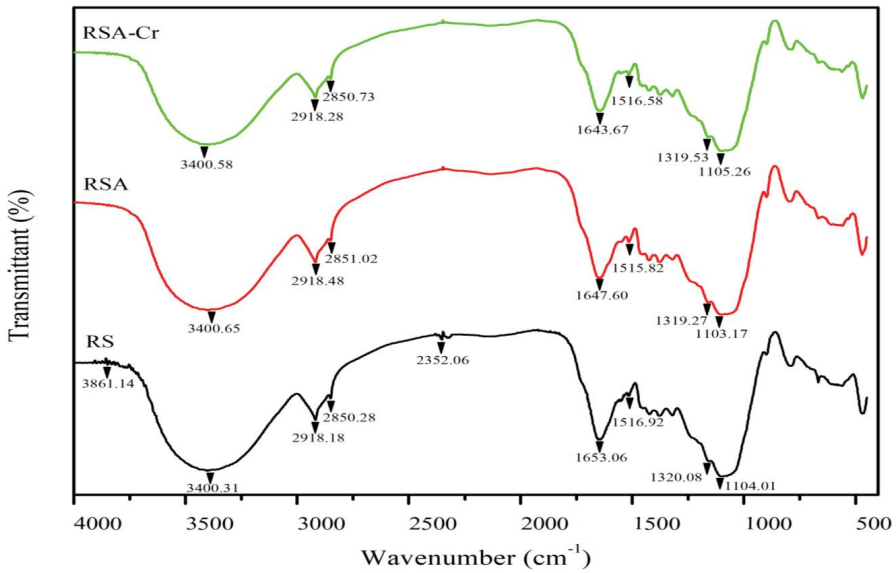

Fig. 1. FTIR spectrum of the activated rice straw for Cr(VI) ion adsorption.

Table 1
Detected functional groups in rice straw

Functional groups	RS (cm^{-1})	RSA (cm^{-1})	RSA-Cr (cm^{-1})
N–H stretching	3,861.14	–	–
Surface O–H stretching	3,400.31	3,400.65	3,400.58
Aliphatic C–H stretching	2,918.03	2,918.48	2,918.28
Aldehyde C–H stretching	2,850.28	–	–
C=O Asymmetric stretching	2,352.06	–	–
Alkene C=C stretching	1,653.06	1,647.60	1,643.67
Aromatic C–NO_2 stretching	1,516.92	1,515.82	1,516.58
Carboxylate anion C=O stretching	1,320.08	1,319.27	1,319.53
Si–O stretching	1,104.51	1,103.17	1,105.26

Table 2
XRF study of rice straw composition

Compound	Before adsorption	After adsorption
	Concentration (%w/w)	Concentration (%w/w)
Mg	1.593	0
Si	50.492	51.846
K	21.232	8.416
Ca	10.766	14.062
Cl	3.234	0.164
MgO	1.923	0
SiO_2	66.19	67.034
K_2O	11.806	4.898
CaO	6.258	8.926
Cr	0	7.015

CrO_4^{2-} and $Cr_2O_7^{2-}$) in solution and bioadsorbent [36,37]. Table 2 also indicates an ion exchange between Cr(VI) and Cl^-. The number of Cr(VI) ions adsorbed was proportional to 2 times the released Cl^- ions. It indicated that the exchange of Cr(VI) ions in solution in the form of CrO_4^{2-} species with Cl^- followed the charge balance reaction rules [Eq. (4)] [38]:

$$2FG\text{-}Cl^- + CrO_4^{2-} \rightarrow \left[FG\right]_2 CrO_4^{2-} + 2Cl^- \quad (4)$$

where FG represented the exchange site on the RSA surface.

3.1.2. SEM-EDX analysis

The surface morphology of activated rice straw was described using the result of SEM examination (1000x magnification). As seen in Fig. 2, activated straw's rough and porous surface has become smoother after the adsorption of Cr(VI) ions. This phenomenon revealed that Cr(VI) ions had covered the bioadsorbent surface. In agreement with other references, the smoother surface structure was due to the reduction of cellulose, hemicellulose lignin, and others and the addition of particles or metal ions on the surface of the bioadsorbent [16,18].

Meanwhile, the EDX spectrum proved that Cr(VI) ions had coated the surface of the activated rice straw. It indicated that chemical interactions have occurred through complex formation, ion exchange, electrostatic interactions, or through pores between Cr(VI) ions and the bioadsorbent [39].

3.1.3. TGA analysis

TGA analysis was conducted to determine the thermal stability of activated rice straw. As shown in Fig. 3, Cr(VI) ion adsorption capacity dropped from 60.94 to 16.91 mg/g along with the increase in temperature from 25 to 250°C, due to the decomposition of chemical compounds in activated rice straw. The stability of bioadsorbent decreased

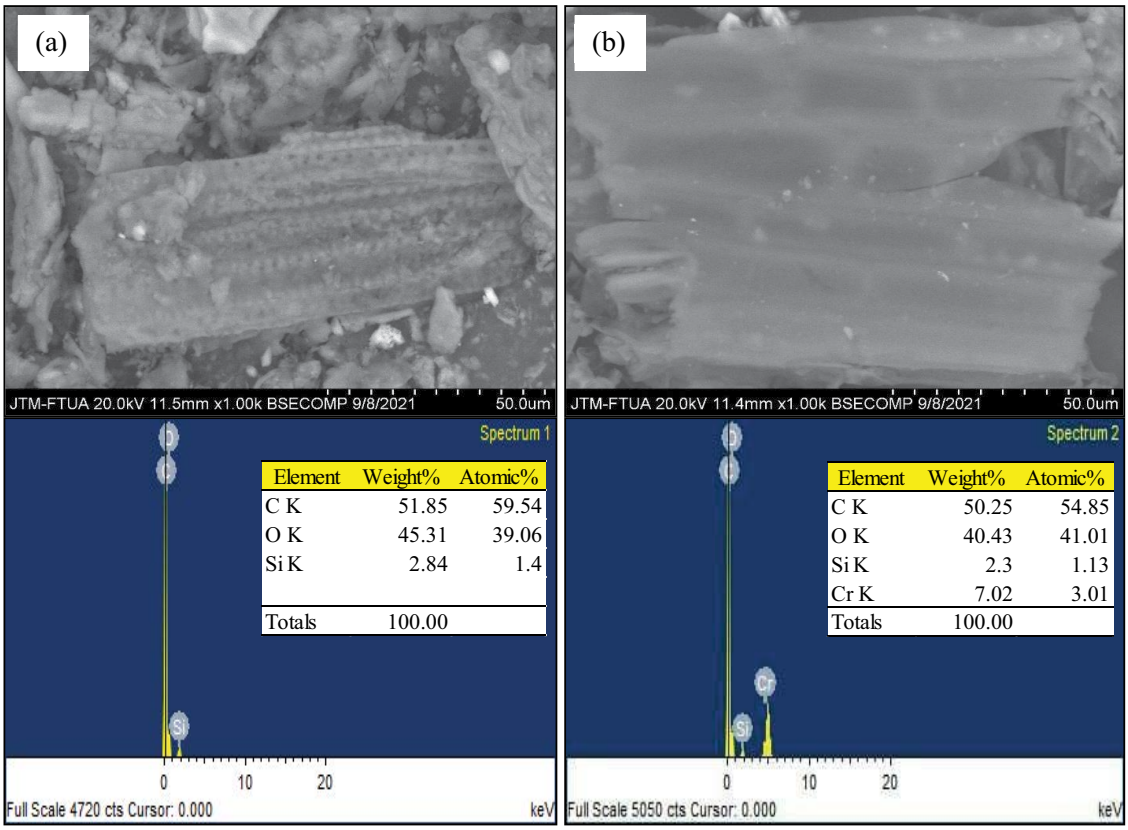

Fig. 2. SEM-EDX of activated rice straw, (a) before Cr(VI) ions adsorption and (b) after Cr(VI) ions adsorption (magnification 1,000×).

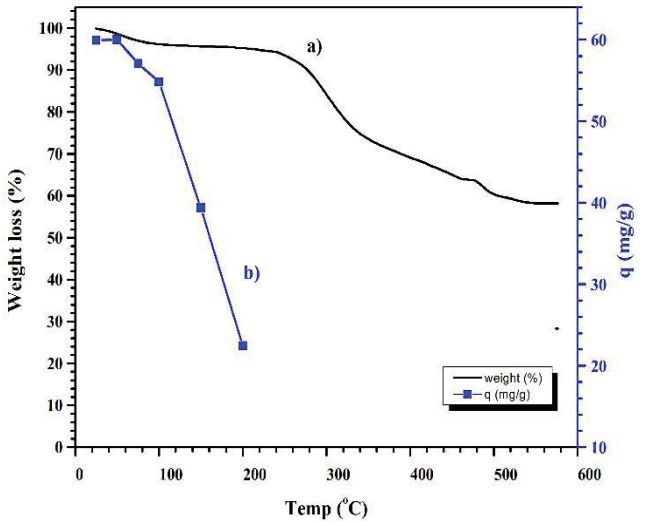

Fig. 3. (a) TGA curve and (b) effect of heating temperature-activated rice straw behavior on Cr(VI) ions removal; initial concentration of 800 mg/L, pH 3, a mass of bioadsorbent 0.1 g and stirring speed of 100 rpm, contact time of 15 min.

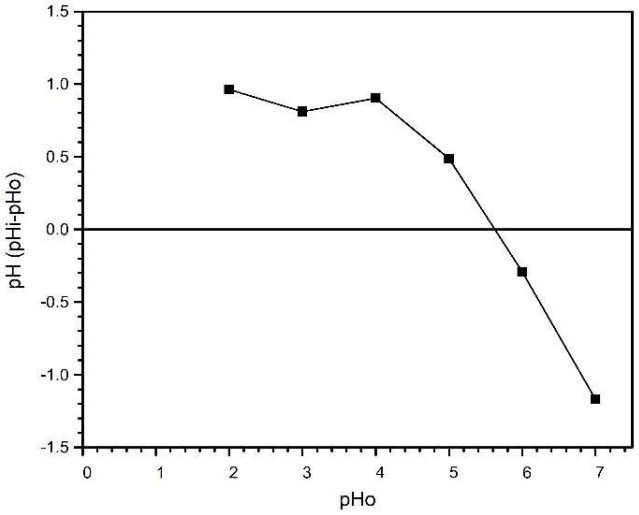

Fig. 4. pH_{pzc} of activated rice straw.

significantly at the temperature of around 250°C. It might be due to the main components that made up activated rice straw such as cellulose, hemicellulose, lignin, silica were damaged [25,40]. Therefore, the decomposition of carboxyl and hydroxyl groups caused glycoside bonds to break and the initiation of breaking of C=O and C–C bonds. When the crystal structure of the compound was damaged, the degree of polymerization decreased, so the activated rice straw experienced the highest mass loss at the temperature of 400°C. When the temperature reached 500°C, an aromatic ring developed, followed by the development of a graphite structure. The residual mass did not change further [41].

3.2. Biosorption study

3.2.1. Point zero charge and the effects of pH on adsorption

pH_{pzc} was an important function of physicochemical characterization that predicted the point where the number of positive and negative charges were equal. The data show that pH_{pzc} of activated rice straw was reached at pH 5.7 (Fig. 4). This was suggested that the bioadsorbent surface was positively charged at the pH < pH_{pzc} due to the protonation of the functional groups. While the pH value was above pH_{pzc}, the bioadsorbent surface was negatively charged due to the deprotonation of the functional groups [42].

pH played a significant role in adsorption. pH affected the interaction between bioadsorbent and Cr(VI) ions related to the surface charge of bioadsorbent. The maximum adsorption capacity of Cr(VI) removal was reached at pH 3. When pH < 3, the adsorbent surface was positively charged due to the protonation of hydrogen ion in the solution. This phenomenon induced electrostatic interaction between activated rice straw and chromium ion's species consisting of $HCrO_4^-$, CrO_4^{2-}, and $Cr_2O_7^{2-}$ [28,43].

Meanwhile, at pH > 3, Cr(VI) ion adsorption capacity reduced from 0.524 to 0.018 mg/g due to the high number of negatively charged OH^- ions on the surface of the bioadsorbent, resulting in a repulsion force between the oxy-anions and the surface of the bioadsorbent. This was also related to the pH_{pzc} value of the activated bioadsorbent, where the condition of providing the bioadsorbent charge was at pH 5.7. If the pH of the Cr(VI) ion solution approached the pH_{pzc} of bioadsorbent, the surface of the bioadsorbent tended to come neutral due to deprotonation of the functional group (Fig. 5) [42].

3.2.2. Effect of Cr(VI) ion concentration and equilibrium study

Effect of initial concentration of Cr(VI) ion was evaluated within the range of 100–1,200 mg/L at 25°C. When the initial concentration of Cr(VI) increased from 100–800 mg/L, the adsorption capacity of activated rice straw increased from 0.804 to 60.204 mg/g because of the large number of active sited availability. The greater the initial concentration, the greater the mass transfer driving force, which overcame the barrier of Cr(VI) ions from the liquid phase to the bioadsorbent surface. Thus, the adsorption rate was almost directly proportional to the increase in the initial concentration of Cr(VI) ions. Then the number of active sites available would gradually decrease, so the adsorption rate became slower until it reached equilibrium. At the higher concentration, the rate of adsorption decreased because the active site on the outer surface has been saturated and occupied by metal ions on the surface of the bioadsorbent, causing a decrease in the adsorption capacity of Cr(VI) ions, due to competition to occupy the active sites [31,44,45]. The adsorption peak condition was obtained at the concentration of 800 mg/L with an adsorption capacity of 60.20 mg/g (Fig. 6).

Langmuir and Freundlich isotherms models were used to investigate the equilibrium adsorption of Cr(VI) with activated rice straw. Adsorption was believed to be restricted to monolayer coverage in the Langmuir isotherm

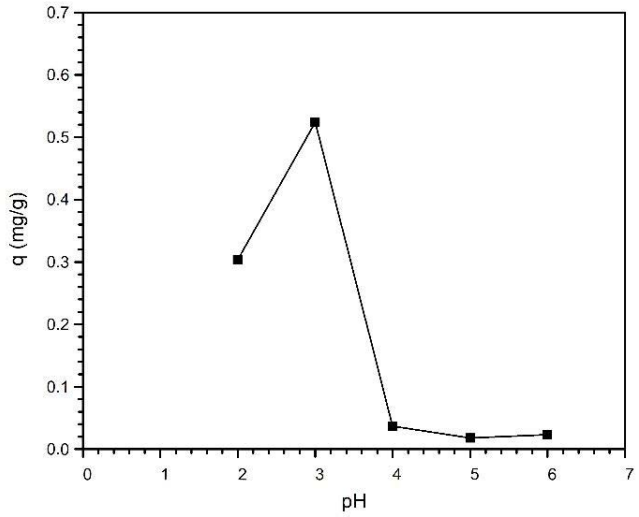

Fig. 5. Effect of pH on the adsorption of Cr(VI) ions with activated rice straw; initial concentration of 10 mg/L, a mass of bioadsorbent 0.1 g, particle size ≥36 μm, contact time 60 min, temperature 25°C and stirring speed 100 rpm.

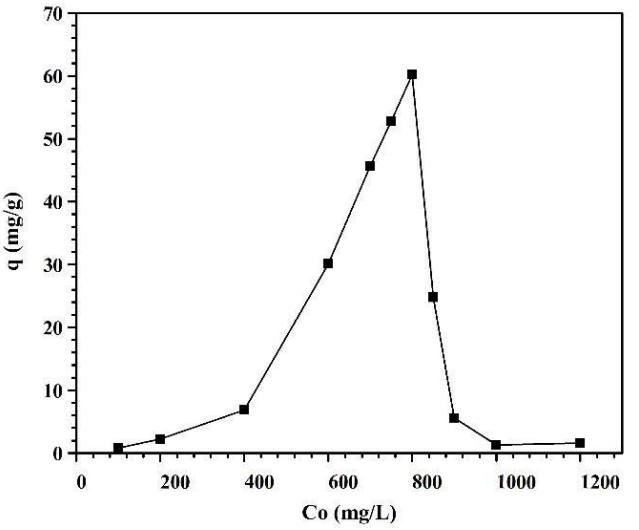

Fig. 6. Effect of the initial concentration of Cr(VI) ions on adsorption with activated rice straw; initial concentration 100–1,200 mg/L, pH 3, bioadsorbent mass 0.1 g, contact time 60 min, temperature 25°C, and stirring speed 100 rpm.

model. The active site was only able to bind one adsorbate atom, and the ability of the molecule to adsorb to the active site was not affected by environmental conditions [46,47]. The Langmuir isotherm model was expressed by the following Eq. (5):

$$\frac{C_e}{q_e} = \frac{1}{q_m \cdot K_L} + \frac{C_e}{q_m} \tag{5}$$

where C_e was the concentration at the equilibrium (mg/L), q_e was adsorption capacity at equilibrium (mg/g), q_m was maximum adsorption capacity (mg/g), and K_L was Langmuir constant (L/mg).

The separation factor (R_L) was an important the Langmuir isotherm's defining feature. The form of the equation is shown in Eq. (6).

$$R_L = \frac{1}{1 + K_L \cdot C_o} \tag{6}$$

where K_L was the Langmuir constant, C_o was the initial concentration of metal ions. This separation factor (R_L) indicated whether or not the adsorption process was favorable. If the value of $R_L = 0$, the adsorption process tended to be irreversible. R_L ($0 < R_L < 1$), the adsorption process tended to be favorable, if $R_L = 1$, the adsorption process was linear, and if $R_L > 1$, the adsorption was unfavorable [46]. The result shows that R_L value of Cr(VI) sorption onto activated rice straw was 1 revealing a linear process.

While the Freundlich isotherm models assumed that the active sites were exponentially distributed with the heat of adsorption [46]. The Freundlich isotherm model is expressed by Eq. (7):

$$\log q_e = \log K_F + \frac{1}{n} \log C_e \tag{7}$$

where q_e was adsorption capacity at equilibrium (mg/g), K_F was Freundlich constant (L/mg), and $1/n$ was the adsorption intensity. Table 3 shows that the adsorption constant (n_F) tended to be favorable because the n_F value was in the range of $0.1 < 1/n < 1$.

Fig. 7 indicates the coefficient determination of the Langmuir isotherm model (R^2 = 0.6285) and Langmuir constant (K_L = 0.0186). Langmuir constant (K_L) showed the affinity of heavy metals toward bioadsorbent. The R^2 value of the Freundlich isotherm model (R^2 = 0.9957) was higher than the Langmuir isotherm model and close to 1. Therefore, the adsorption process of Cr(VI) onto activated rice straw followed the Freundlich isotherm model indicating multilayer adsorption process on the heterogeneous surface and heterogeneous energy of the active site. Similar results have been reported by other literature [46,47].

Dubinin–Radushkevich's isotherm model could predict how adsorbate entered adsorbent's pores with Gaussian energy distribution on heterogeneous surfaces [48]. The linear and non-linear form of the Dubinin–Radushkevich isotherm model were calculated by Eqs. (8)–(11):

$$q_e = q_m \exp\left(-K\varepsilon^2\right) \tag{8}$$

$$\ln q_e = \ln q_m \left(-K\varepsilon^2\right) \tag{9}$$

$$\varepsilon = RT \ln\left(1 + \frac{1}{C_e}\right) \tag{10}$$

$$E_{\mathrm{DR}} = \left(2K_{\mathrm{DR}}\right)^{-0.5} \tag{11}$$

Table 3
Parameters of isotherm model on the adsorption of Cr(VI) ions

Isotherm models	Results
Langmuir	
K_L (L/mg)	0.0186
$q_{m,calc}$ (mg/g)	61.349
R_L	1
R^2	0.6285
Freundlich	
K_F (L/g)	1.1256
n_F	1.0551
R^2	0.9957
Dubinin–Radushkevich	
$q_{m,calc}$ (mg/g)	6.6667
K_{DR} (mol^2/kJ)	6×10^{-7}
E_{DR} (kJ/mol)	2.8867
R^2	0.8423

where q_m indicates the saturation capacity of the theoretical Dubinin–Radushkevich isotherm (mg/g). K_{DR} is the isotherm constant Dubinin–Radushkevich (mol^2/kJ), ε is the Polanyi potential associated with equilibrium concentration, and E_{DR} is the average free energy of adsorption (kJ/mol).

Dubinin–Radushkevich isotherm models (Table 3). If E_{DR} was within the range of 8–16 kJ/mol, the adsorption has chemically occurred. If E_{DR} > 16 kJ/mol indicated a diffusion process and If E_{DR} < 8 kJ/mol revealed that the adsorption process has physically occurred [49]. In this research, the E_{DR} value was 2.88 kJ/mol representing physisorption and multilayer adsorption involving Van der Waal force [50]. According to previous research of Khalil et al. [51], lower E_{DR} pointed out that Dubinin–Radushkevich was not suitable to describe the adsorption process of Cr(VI) onto activated rice straw.

3.2.3. Effect of contact time and kinetic study

The effect of contact time on the adsorption process aimed to determine the minimum time required by activated rice straw for removing Cr(VI) ions. Fig. 8 shows the

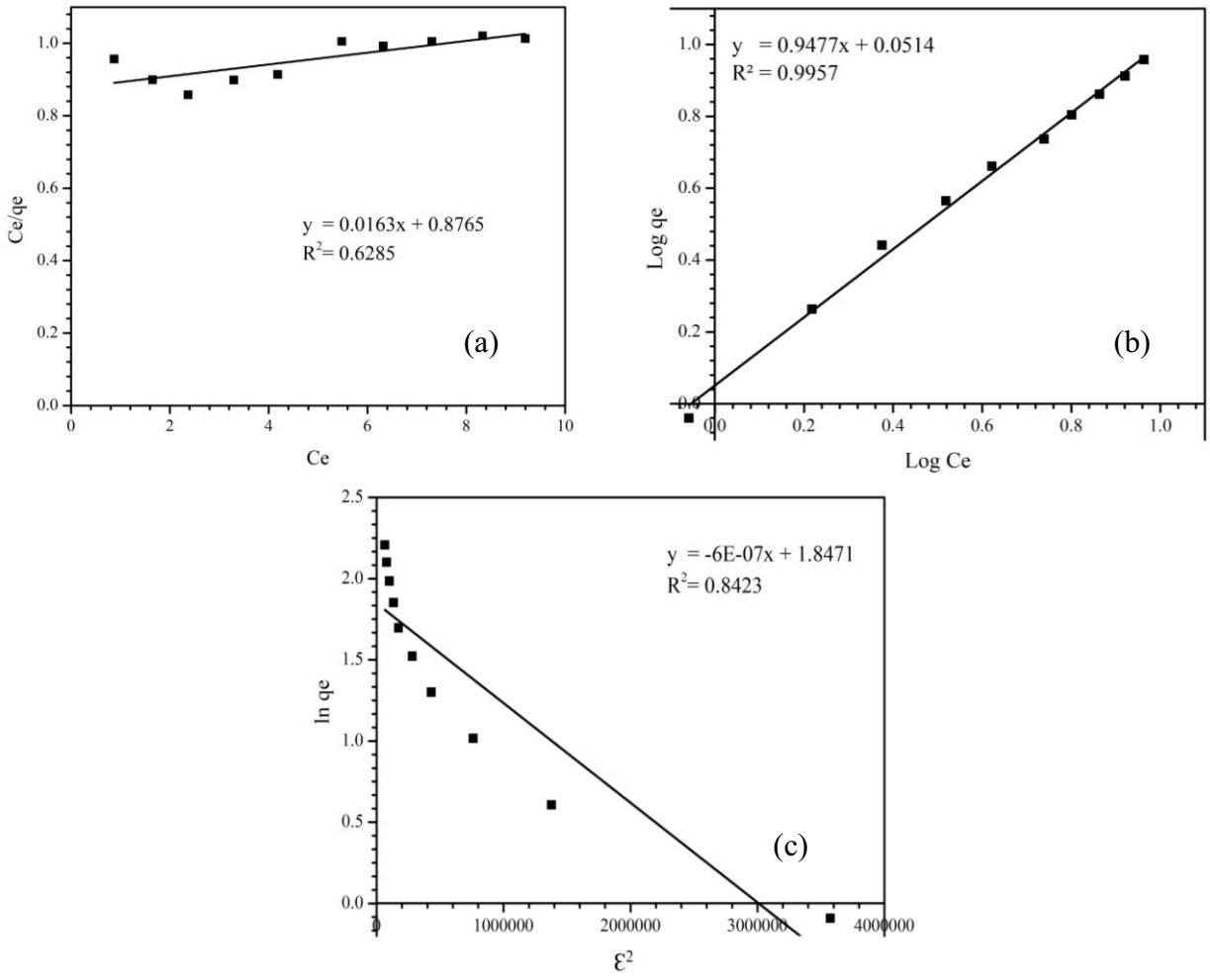

Fig. 7. The adsorption isotherm models of Cr(VI) ions adsorption onto activated rice straw: (a) Langmuir, (b) Freundlich, and (c) Dubinin–Radushkevich.

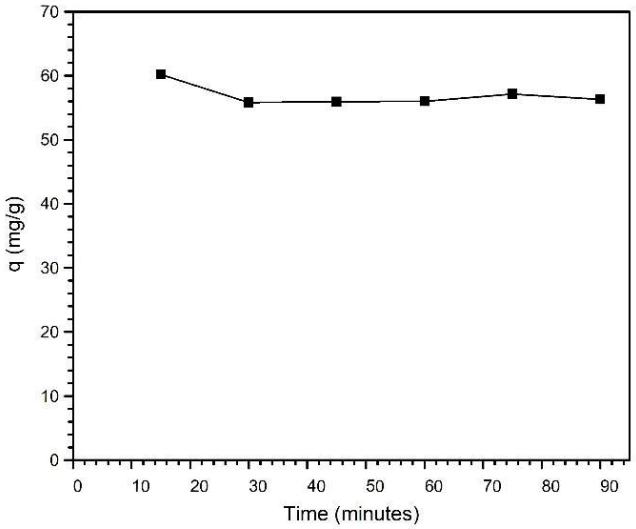

Fig. 8. Effect of contact time on the adsorption of Cr(VI) ions with activated rice straw; initial concentration of 800 mg/L, pH 3, a mass of bioadsorbent 0.1 g, and stirring speed of 100 rpm.

optimum condition for Cr(VI) ions removal using activated rice straw was obtained within 15 min at the temperature of 25°C with an adsorption capacity of 60.18 mg/g. This condition was related to the availability of active sites that have not been occupied, making it easier for Cr(VI) ions to interact with bioadsorbent [44]. Then the availability of active sited was reduced as time increased leading the adsorption capacity to decline due to a weak bond between bioadsorbent and adsorbate [52].

The behavior of Cr(VI) adsorption onto activated rice straw was evaluated using pseudo-first-order, pseudo-second-order, and Weber–Morris (Table 4). The pseudo-first-order model assumed a liquid-solid system based on solid capacity and a linear plot can be achieved by Eq. (12) [53]:

$$\log\left(q_e - q_t\right) = \log q_e - \frac{k_1}{2.303}t \tag{12}$$

where k_1 was a pseudo-first-order reaction rate constant (1/min), t was a time (min), q_e was the number of metal ions adsorbed at equilibrium (mg/g), q_t was the number of metal ions adsorbed at the certain time (mg/g).

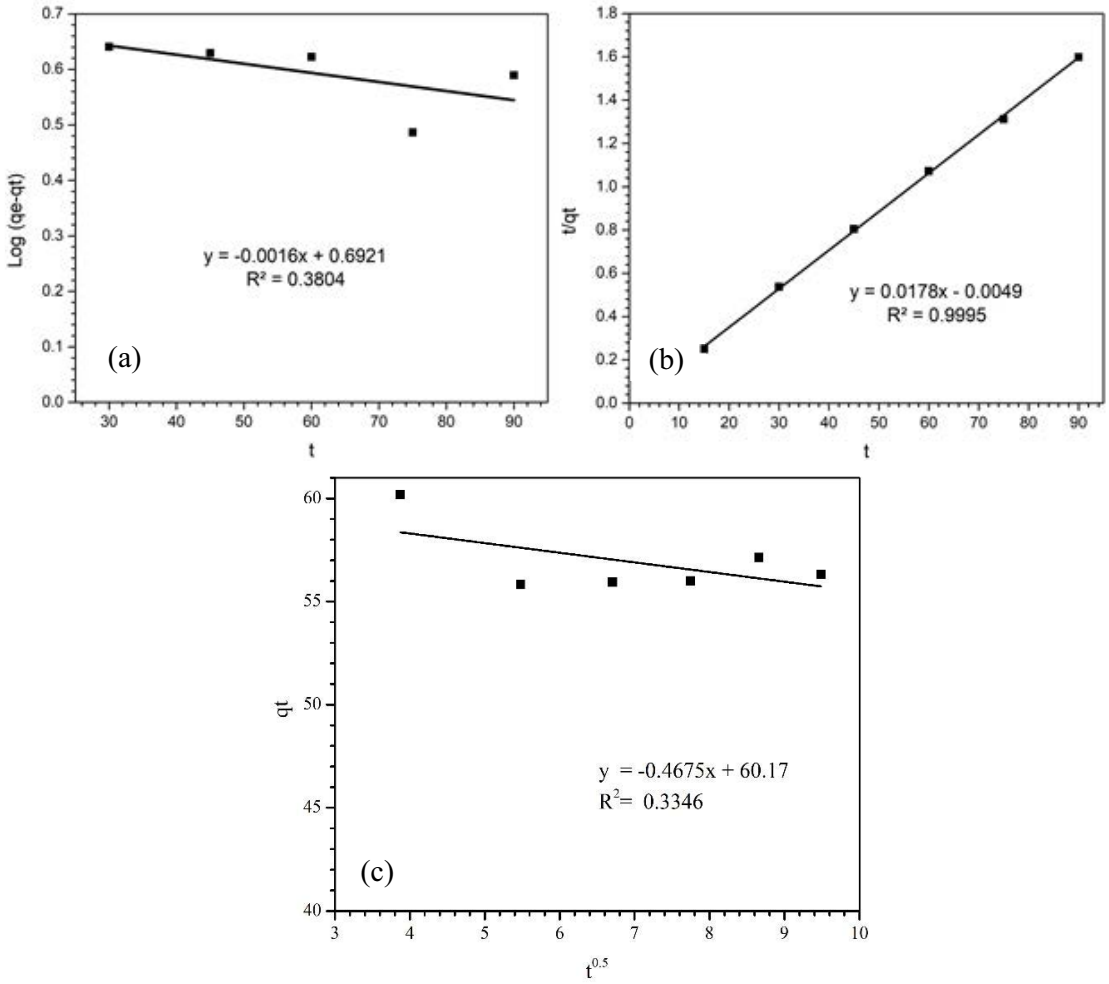

Fig. 9. The kinetic model of Cr(VI) ions adsorption onto activated rice straw (a) pseudo-first-order, (b) pseudo-second-order, and (c) Weber–Morris.

Table 4
Kinetic parameters of Cr(VI) ions adsorption onto activated rice straw

Kinetic models	Equations	Results
Pseudo-first-order	$\log(q_e - q_t) = \log q_e - \frac{k_1}{2.303}t$	
k_1 (min^{-1})		0.0037
$q_{e,calc}$ (mg/g)		0.2030
R^2		0.3804
Pseudo-second-order	$\frac{t}{q_t} = \frac{1}{k_2 q_e^2} + \frac{1}{q_e}t$	
k_2 (min^{-1})		0.0647
$q_{e,calc}$ (mg/g)		56.1801
R^2		0.9995
Intraparticle diffusion	$q_t = K_{diff}t^{0.5} + C$	
C		60.17
K_{diff} (mg/g min$^{0.5}$)		–0.4675
R^2		0.6173

The pseudo-second-order model assumed that the adsorption capacity was proportional to the number of active sites contained in the bioadsorbent. The linear equation is shown by Eq. (13):

$$\frac{t}{q_t} = \frac{1}{k_2 q_e^2} + \frac{1}{q_e}t \quad (13)$$

where k_2 was the pseudo-second-order rate constant (g/mg min).

The Weber–Morris kinetic model assumed that the adsorption process occurred due to adsorbate's movement into bioadsorbent surface then diffused into bioadsorbent's pores [54]. Weber–Morris kinetic model can be represented by Eq. (14):

$$q_t = K_{diff}t^{0.5} + C \quad (14)$$

where K_{diff} was diffusion rate constant (g/mg min$^{0.5}$), C was the absorption capacity (mg/g). In Table 4, the determination coefficient of pseudo-first-order and Weber–Morris kinetic models were 0.3804 and 0.6173, respectively (Fig. 9). Those values pointed out that Cr(VI) adsorption onto activated rice straw did not follow both models. It meant that intraparticle diffusion was not a rate-limiting step but also influenced by adsorbent structure, physical and chemical properties of sorbent and adsorbate, interaction, and condition of the system [55]. Whereas, the determination coefficient of pseudo-second-order was 0.9995, revealing that the adsorption of Cr(VI) onto activated rice husk was chemisorption.

3.2.4. Thermodynamic study

The impact of temperature on the adsorption of Cr(VI) ions was investigated within the range of 298–318 K, at the different concentrations of Cr(VI) ion (10–50 mg/L), adsorbent mass 0.1 g, contact time 15 min, and stirring speed 100 rpm. The experimental data showed that the adsorption capacity of activated rice straw increased as the temperature increased from 298 to 318 K. This indicated that the adsorption process of Cr(VI) ions with activated rice straw was exothermic (Table 5).

Table 5
Thermodynamic parameter of Cr(VI) ions adsorption onto activated rice straw

T (K)	$\Delta H°$ (kJ/mol)	$\Delta S°$ (kJ/mol K)	$\Delta G°$ (kJ/mol)
298			10.800
308	–8.658	–65.297	11.453
318			12.106

Thermodynamic parameters confirmed the fact that the reaction was exothermic in nature as indicated by $\Delta H°$ (–). While the value of $\Delta S°$ (–) indicated an increase in affinity. Rice straw was activated for Cr(VI) ions sorption and irregularities at the solid/liquid interface during the adsorption process and the $\Delta G°$ (+) value indicated that the adsorption was not spontaneous. In addition, $\Delta G°$ increased with increasing temperature, this indicated that at high temperatures the adsorption process was favorable [45].

3.2.5. Comparison of adsorption capacity of Cr(VI) ion with other bioadsorbents

Table 6 shows the comparison of Cr(VI) sorption using various adsorbents from previous research with current research. The result indicated that activated rice straw has a higher adsorption capacity than other adsorbents.

3.2.6. Mechanisms of Cr(VI) adsorption onto activated rice straw

The mechanism of Cr(VI) ion adsorption with activated rice straw is described in Fig. 10. The possible mechanisms of Cr(VI) ions removal by activated rice straw were including electrostatic interaction [56], reduction [57,58], complex [59], ion exchange [37,38] and pore adsorption [28,39].

The pH_{zpc} of activated rice straw was reached at pH 5.7, and the optimum pH for Cr(VI) ion adsorption was reached at pH 3. These conditions indicated that at low pH, the surface of the bioadsorbent was protonated and the species $Cr_2O_7^{2-}$, $HCrO_4^-$ was dominant in the solution. Moreover, it allowed for electrostatic interactions between activated rice straw and Cr(VI) ions [31]. The presence of functional groups (electron donors), especially those containing oxygen such as carboxyl and hydroxyl groups, have lower reduction potential on the surface of the bioadsorbent, can cause Cr(VI) (anion) ions to be reduced to Cr(III)(cations) [60]. The carboxyl functional group, hydroxyl, which was negatively charged, could bind Cr(III) through a complexation process on the surface of the bioadsorbent [20]. On the other hand, Ca, Mg, K attached to the surface of the bioadsorbent as a cation-forming agent could cause cation exchange between Ca^{2+}, Mg^{2+}, K^+ and

Table 6
Comparison of adsorption capacity of Cr(VI) ions onto various bioadsorbents

Adsorbent	q_m (mg/g)	References
Neem bark powder	41.67	[11]
Aminated rice straw-grafted-poly(vinyl alcohol) (A-RS/PVA)	34.90	[12]
Mucilaginous seeds of *Cydonia oblonga*	33.58	[13]
Amine-functionalized modified rice straw	15.82	[14]
Bauhinia rufescens plant	9.76	[15]
Biochar from sagwan wood sawdust	9.62	[16]
Magnolia leaf	3.96	[17]
Rice straw	12.17	[25]
Rice bran	12.34	
Rice husk	11.40	
Hyacinth roots	15.28	
Neem leaves	15.95	
Coconut shell	18.69	
Activated rice straw	60,204	This study

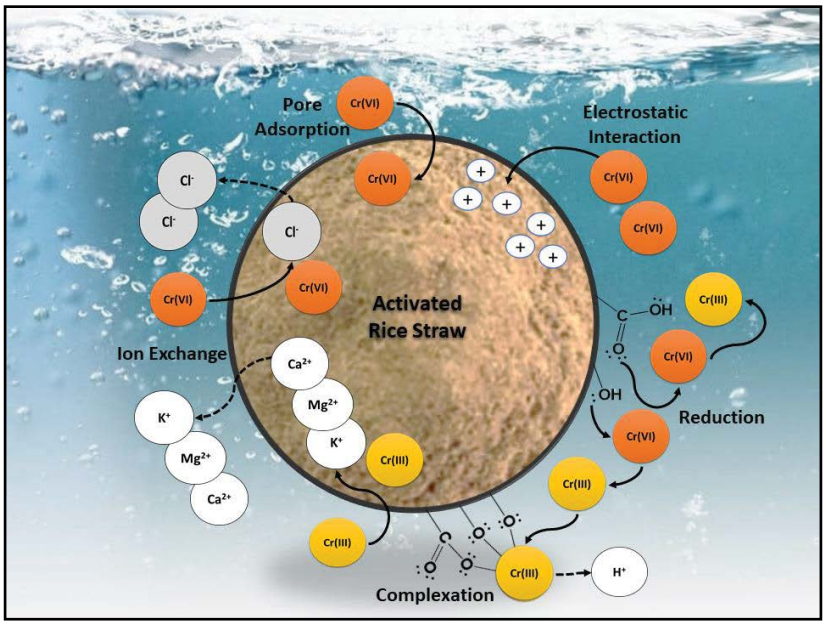

Fig. 10. Cr(VI) ions adsorption mechanism onto activated rice straw.

dissolved Cr(III) [60]. Also, the anion exchange between Cr(VI) and Cl^-, following the rules of the charge balance reaction [Eq. (4)], where the Cr(VI) ion in solution is the species CrO_4^{2-}, adsorbed was proportional to 2 times the Cl^- ions released [38]. This fact was also confirmed by XRF analysis (Table 2). The kinetic model proved that Cr(VI) adsorption onto activated rice straw was chemisorption with intraparticle diffusion rate-limiting step involving exchanging electron/sharing electron between adsorbate and bioadsorbent [61]. While the isotherm model described the adsorption of Cr(VI) onto activated rice straw as physisorption and chemisorption [46].

Characterization using FTIR, XRF, and SEM-EDX also supports this mechanism. Due to the adsorption process, the wavenumbers of several functional groups such as O–H, C=C, C=O, C=O, C–NO_2, Si–O, and C–H. Although the shift is not significant, this finding indicated that the vibrational energy of the functional group has shifted. XRF analysis also proved a change in the chemical composition of activated rice straw, where there was an addition of Cr elemental composition and a decrease in Cl element after adsorption (Table 2). The results of SEM-EDX analysis (Fig. 2) confirmed a change in the surface morphology of the bioadsorbent before and after the adsorption. The surface of the bioadsorbent after adsorption was smoother than before adsorption. And the appearance of Cr peaks in the EDX analysis spectrum proved the occurrence of physical adsorption or pores on the surface of activated

rice straw. Thus, the mechanism of Cr(VI) ion adsorption onto activated rice straw could occur physically and chemically [62].

4. Conclusion

Adsorption of Cr(VI) onto activated rice straw has been successfully conducted. The adsorption reached the peak at the pH 3, Cr(VI) concentration 800 mg/L in 15 min with adsorption capacity 60.20 mg/g. The adsorption process followed Freundlich isotherm model and pseudo-second-order model indicating multilayer adsorption. Cr(VI) covered bioadsorbent surface and confirmed a chemisorption process. Thermodynamic investigation showed that Cr(VI) sorption onto activated rice straw was non-spontaneous, exothermic and the disorder on bioadsorbent surface decreased. Thus, it can be concluded that activated rice straw was efficient, effetive, abundant, simple, and low-cost bioadsorbent for Cr(VI) removal.

Acknowledgment

The authors would like to thank "Directorate of Research and Community Service, Deputy of Research and Development Strengthening of Ministry of Research and Technology/National Research and Innovation Agency" for the financial assistance provided by the terms of agreement DRPM No. 104/E4.1/AK.04.PT/2021, LPPM No. T/10/UN.16.17/PT.01.03/PDD-Material Maju /2021.

References

[1] M.R. Razak, A.Z. Aris, N.A.C. Zakaria, S.Y. Wee, N.A.H. Ismail, Accumulation and risk assessment of heavy metals employing species sensitivity distributions in Linggi River, Negeri Sembilan, Malaysia, Ecotoxicol. Environ. Saf., 211 (2021) 111905, doi: 10.1016/j.ecoenv.2021.111905.

[2] J. Singh, P. Yadav, A.K. Pal, V. Mishra, Water Pollutants: Origin and Status, D. Pooja, P. Kumar, P. Singh, S. Patil, Eds., Water Pollutants Monitoring: Role of Material, Advanced Functional Materials and Sensors, Springer Nature Singapore Pte Ltd., Singapore, 2020, pp. 5–20.

[3] C.L. Rollinson, Chapter 2 – Chromium Compounds, A.F. Trotman-Dickenson, Ed., The Chemistry of Chromium, Molybdenum and Tungsten: Pergamon International Library of Science, Technology, Engineering and Social Studies, Pergamon Press Ltd., England, 1973, pp. 623–664.

[4] Florenly, E. Fachrial, H. Aziz, Syafrizayanti, R. Zein, The effects of Cr(VI) in the kidney of experimental rats and utilization of longanpeel fruit (*Dimocarpuslongan*) as renal protector in dentistry, Der Pharma Chem., J. Med. Chem. Pharm. Chem. Pharm. Sci. Comput. Chem., 8 (2016) 144–148.

[5] S.B. Abadin, H. Fay, M. Ingerman, L. Tencza, B. Yu, D. Wilbur, Toxicological Profile for Chromium, Atlanta, 2012.

[6] WHO, Chromium in Drinking-Water, Background Document for Development of WHO Guidelines for Drinking-Water Quality, Geneva, Switzerland, 2020.

[7] Menteri Kesehatan Republik Indonesia, Peraturan Menteri Kesehatan Republik Indonesia Nomor 32 Tahun 2017 Tentang Standar Baku Mutu Kesehatan Lingkungan Dan Persyaratan Kesehatan Air Untuk Keperluan Higiene Sanitasi, Kolam Renang, Solus Per Aqua dan Pemandian Umum, Peratur, Menteri Kesehat, Republik Indones., 2017, pp. 1–20.

[8] D. Sharma, P.K. Chaudhari, A.K. Prajapati, Removal of chromium(VI) and lead from electroplating effluent using electrocoagulation, Sep. Sci. Technol., 55 (2020) 321–331.

[9] A.S. Dharnaik, P.K. Ghosh, Hexavalent chromium [Cr(VI)] removal by the electrochemical ion-exchange process, Environ. Technol. (United Kingdom), 35 (2014) 2272–2279.

[10] Z. Zhao, H. An, J. Lin, M. Feng, V. Murugadoss, T. Ding, H. Liu, Q. Shao, X. Mai, N. Wang, H. Gu, S. Angaiah, Z. Guo, Progress on the photocatalytic reduction removal of chromium contamination, Chem. Rec., 19 (2019) 873–882.

[11] W. Duan, G. Chen, C. Chen, R. Sanghvi, A. Iddya, S. Walker, H. Liu, A. Ronen, D. Jassby, Electrochemical removal of hexavalent chromium using electrically conducting carbon nanotube/polymer composite ultrafiltration membranes, J. Membr. Sci., 531 (2017) 160–171.

[12] T. Altun, E. Pehlivan, Removal of Cr(VI) from aqueous solutions by modified walnut shells, Food Chem., 132 (2012) 693–700.

[13] R. Zein, D.A. Hidayat, M. Elfia, N. Nazarudin, E. Munaf, Sugar palm *Arenga pinnata* Merr (*Magnoliophyta*) fruit shell as biomaterial to remove Cr(III), Cr(VI), Cd(II) and Zn(II) from aqueous solution, J. Water Supply Res. Technol., 63 (2014) 553–559.

[14] E. Vaiopoulou, P. Gikas, Effects of chromium on activated sludge and on the performance of wastewater treatment plants: a review, Water Res., 46 (2012) 549–570.

[15] M.P.S. Kumar, B.R. Phanikumar, Response surface modelling of Cr^{6+} adsorption from aqueous solution by neem bark powder: Box–Behnken experimental approach, Environ. Sci. Pollut. Res., 20 (2013) 1327–1343.

[16] C. Lin, W. Luo, T. Luo, Q. Zhou, H. Li, L. Jing, A study on adsorption of Cr(VI) by modified rice straw: characteristics, performances and mechanism, J. Cleaner Prod., 196 (2018) 626–634.

[17] E. Bazrafshan, M. Sobhanikia, F.K. Mostafapour, H. Kamani, D. Balarak, Chromium biosorption from aqueous environments by mucilaginous seeds of *Cydonia oblonga*: thermodynamic, equilibrium and kinetic studies, Global Nest J., 19 (2017) 269–277.

[18] Y. Wu, Y. Fan, M. Zhang, Z. Ming, S. Yang, A. Arkin, P. Fang, Functionalized agricultural biomass as a low-cost adsorbent: utilization of rice straw incorporated with amine groups for the adsorption of Cr(VI) and Ni(II) from single and binary systems, Biochem. Eng. J., 105 (2016) 27–35.

[19] O. Alabi, A.A. Olanrewaju, T.J. Afolabi, Process optimization of adsorption of Cr(VI) on adsorbent prepared from *Bauhinia rufescens* pod by Box–Behnken design, Sep. Sci. Technol., 55 (2020) 47–60.

[20] G.K. Gupta, M.K. Mondal, Mechanism of Cr(VI) uptake onto sagwan sawdust derived biochar and statistical optimization via response surface methodology, Biomass Convers. Biorefin., (2020), doi: 10.1007/s13399-020-01082-5.

[21] N.K. Mondal, A. Samanta, P. Roy, B. Das, Optimization study of adsorption parameters for removal of Cr(VI) using Magnolia leaf biomass by response surface methodology, Sustainable Water Resour. Manage., 5 (2019) 1627–1639.

[22] BPS RI, Data BPS Produksi Padi 2019, 2019. Available at: https://www.bps.go.id/

[23] M. Jain, V.K. Garg, K. Kadirvelu, M. Sillanpää, Combined effect of sunflower stem carbon–calcium alginate beads for the removal and recovery of chromium from contaminated water in column mode, Ind. Eng. Chem. Res., 54 (2015) 1419–1425.

[24] R.C. Sun, J. Tomkinson, P.L. Ma, S.F. Liang, Comparative study of hemicelluloses from rice straw by alkali and hydrogen peroxide treatments, Carbohydr. Polym., 42 (2000) 111–122.

[25] S. Mirmohamadsadeghi, K. Karimi, Chapter 21 – Recovery of Silica From Rice Straw and Husk, S. Varjani, A. Pandey, E. Gnansounou, S.K. Khanal, S. Raveendran, Eds., Current Developments in Biotechnology and Bioengineering: Resource Recovery from Wastes, Elsevier, 2020, pp. 411–433.

[26] L. Fu, Y. Liu, Z. Wang, Y. Chen, C. He, Ion adsorption of rice straw to marine heavy metal polluted wastewater, J. Coastal Res., 83 (2018) 359–363.

[27] H. Gao, Y. Liu, G. Zeng, W. Xu, T. Li, W. Xia, Characterization of Cr(VI) removal from aqueous solutions by a surplus agricultural waste—rice straw, J. Hazard. Mater., 150 (2008) 446–452.

[28] W. Cao, Z. Dang, X.Y. Yi, C. Yang, G.N. Lu, Y.F. Liu, S.Y. Huang, L.C. Zheng, Removal of chromium(VI) from electroplating wastewater using an anion exchanger derived from rice straw, Environ. Technol. (United Kingdom), 34 (2013) 7–14.
[29] B. Singha, S.K. Das, Biosorption of Cr(VI) ions from aqueous solutions: kinetics, equilibrium, thermodynamics and desorption studies, Colloids Surf., B, 84 (2011) 221–232.
[30] S. Yakoyama, M. Yukihiko, The Asian Biomass Handbook: A Guide for Biomass Production and Utilization, 1st ed., The Japan Institute of Energy, Japan, 2008.
[31] S. Fauzia, H. Aziz, D. Dahlan, J. Namieśnik, R. Zein, Adsorption of Cr(VI) in aqueous solution using sago bark (metroxylon sagu) as a new potential biosorbent, Desal. Water Treat., 147 (2019) 191–202.
[32] V.C. Srivastava, I.D. Mall, I.M. Mishra, Characterization of mesoporous rice husk ash (RHA) and adsorption kinetics of metal ions from aqueous solution onto RHA, J. Hazard. Mater., 134 (2006) 257–267.
[33] T.A. Davis, B. Volesky, A. Mucci, A review of the biochemistry of heavy metal biosorption by brown algae, Water Res., 37 (2003) 4311–4330.
[34] T.K. Naiya, B. Singha, S.K. Das, FTIR study for the Cr(VI) removal from aqueous solution using rice waste, Int. Proc. Chem. Biol. Environ. Eng., 10 (2011) 114–119.
[35] A.S. Sharma, S.A. Bhalerao, Batch removal of chromium(VI) by biosorption on to banana peels (*Musa Paradisiaca* L.), World Wide J. Multidiscip. Res. Dev., 4 (2018) 5–17.
[36] M. Nigam, S. Rajoriya, S. Rani Singh, P. Kumar, Adsorption of Cr(VI) ion from tannery wastewater on tea waste: kinetics, equilibrium and thermodynamics studies, J. Environ. Chem. Eng., 7 (2019) 103188, doi: 10.1016/j.jece.2019.103188.
[37] A. Dąbrowski, Z. Hubicki, P. Podkościelny, E. Robens, Selective removal of the heavy metal ions from waters and industrial wastewaters by ion-exchange method, Chemosphere, 56 (2004) 91–106.
[38] W. Cao, Z. Dang, G.N. Lu, Kinetics and mechanism of Cr(VI) Sorption from aqueous solution on a modified lignocellulosic material, Environ. Eng. Sci., 30 (2013) 672–680.
[39] H. Li, X. Dong, E.B. da Silva, L.M. de Oliveira, Y. Chen, L.Q. Ma, Mechanisms of metal sorption by biochars: biochar characteristics and modifications, Chemosphere, 178 (2017) 466–478.
[40] I. Barmina, A. Lickrastina, R. Valdmanis, M. Zake, A. Arshanitsa, V. Solodovnik, G. Telysheva, Effects of biomass composition variations on gasification and combustion characteristics, Eng. Rural Dev., (2013) 382–387.
[41] Y. Feng, Y. Liu, L. Xue, H. Sun, Z. Guo, Y. Zhang, L. Yang, Carboxylic acid functionalized sesame straw: a sustainable cost-effective bioadsorbent with superior dye adsorption capacity, Bioresour. Technol., 238 (2017) 675–683.
[42] N.D. Shooto, Removal of toxic hexavalent chromium (Cr(VI)) and divalent lead (Pb(II)) ions from aqueous solution by modified rhizomes of *Acorus calamus*, Surf. Interfaces, 20 (2020) 100624, doi: 10.1016/j.surfin.2020.100624.
[43] K. Legrouri, E. Khouya, H. Hannache, M. El Hartti, M. Ezzine, R. Naslain, Activated carbon from molasses efficiency for Cr(VI), Pb(II) and Cu(II) adsorption: a mechanistic study, Chem. Int., 3 (2017) 301–310.
[44] Z. Chaidir, R. Zein, Q. Hasanah, H. Nurdin, H. Aziz, Absorption of Cr(III) and Cr(VI) metals in aqueous solution using Mangosteen Rind (*Pithecellobium jiringa* (jack) prain.), J. Chem. Pharm. Res., 7 (2015) 948–956.
[45] X. Shi, Y. Qiao, X. An, Y. Tian, H. Zhou, High-capacity adsorption of Cr(VI) by lignin-based composite: characterization, performance and mechanism, Int. J. Biol. Macromol., 159 (2020) 839–849.
[46] M. Kumar, R. Tamilarasan, Kinetics, equilibrium data and modeling studies for the sorption of chromium by *Prosopis juliflora* bark carbon, Arabian J. Chem., 10 (2017) S1567–S1577.
[47] I. Langmuir, The adsorption of gases on plane surfaces of glass, mica and platinum, J. Am. Chem. Soc., 40 (1918) 1361–1403.
[48] N. Ayawei, A.N. Ebelegi, D. Wankasi, Modelling and interpretation of adsorption isotherms, J. Chem., 2017 (2017) 1–11.
[49] D. Balarak, M. Baniasadi, S. Lee, M.J. Shim, Ciprofloxacin adsorption onto *Azolla filiculoides* activated carbon from aqueous solutions, Desal. Water Treat., 218 (2021) 444–453.
[50] U. Israel, U.M. Eduok, Biosorption of zinc from aqueous solution using coconut (*Cocos nucifera* L) coir dust, Sch. Res. Libr. Arch. Appl. Sci. Res., 4 (2012) 809–819.
[51] U. Khalil, M. Bilal Shakoor, S. Ali, M. Rizwan, M. Nasser Alyemeni, L. Wijaya, Adsorption-reduction performance of tea waste and rice husk biochars for Cr(VI) elimination from wastewater, J. Saudi Chem. Soc., 24 (2020) 799–810.
[52] R. Zein, S. Syukri, M. Muhammad, I. Pratiwi, D.R. Yutaro, The ability of Pensi (*Corbicula moltkiana*) shell to adsorb Cd(II) and Cr(VI) ions, AIP Conf. Proc., 2023 (2018) 020099.
[53] G.M.Y.S. Ho, Pseudo-second-order model for sorption processes, Process Biochem., 34 (1999) 451–465.
[54] W.J. Weber, J.C. Morris, Kinetics of adsorption on carbon from solution, J. Sanit. Eng. Div., 89 (1963) 31–59.
[55] A. Pholosi, E.B. Naidoo, A.E. Ofomaja, Intraparticle diffusion of Cr(VI) through biomass and magnetite coated biomass: a comparative kinetic and diffusion study, S. Afr. J. Chem. Eng., 32 (2020) 39–55.
[56] K.K. Singh, R. Rastogi, S.H. Hasan, Removal of Cr(VI) from wastewater using rice bran, J. Colloid Interface Sci., 290 (2005) 61–68.
[57] M.H. Gonzalez, G.C.L. Araújo, C.B. Pelizaro, E.A. Menezes, S.G. Lemos, G.B. de Sousa, A.R.A. Nogueira, Coconut coir as biosorbent for Cr(VI) removal from laboratory wastewater, J. Hazard. Mater., 159 (2008) 252–256.
[58] K.M.S. Sumathi, S. Mahimairaja, R. Naidu, Use of low-cost biological wastes and vermiculite for removal of chromium from tannery effluent, Bioresour. Technol., 96 (2005) 309–316.
[59] F. Gode, E.D. Atalay, E. Pehlivan, Removal of Cr(VI) from aqueous solutions using modified red pine sawdust, J. Hazard. Mater., 152 (2008) 1201–1207.
[60] T. Chen, Z. Zhou, S. Xu, H. Wang, W. Lu, Adsorption behavior comparison of trivalent and hexavalent chromium on biochar derived from municipal sludge, Bioresour. Technol., 190 (2015) 388–394.
[61] T. Brahmaiah, L. Spurthi, K. Chandrika, S. Ramanaiah, K.S. Sai Prasad, Kinetics of heavy metal (Cr & Ni) removal from the wastewater by using low-cost adsorbent, World J. Pharm. Pharm. Sci., 4 (2015) 1600–1610.
[62] M. Sulyman, J. Namiesnik, A. Gierak, Low-cost adsorbents derived from agricultural by-products/wastes for enhancing contaminant uptakes from wastewater: a review, Polish J. Environ. Stud., 26 (2017) 479–510.